

Full Length Research Paper

# Synthesis and magnetic characterization of $ZnMnO_3$ nanoparticles

Enzo Hernández\* and Vicente Sagredo

Magnetism Laboratory, Department of Physics, Faculty of Science, 5101 University of Los Andes, Merida, Venezuela.

Received 1 April, 2015; Accepted 26 June, 2015

$ZnMnO_3$  nanoparticles system was prepared by the sol-gel auto-combustion method, in order to analyze the structure and magnetic behavior presented in such compound prepared by a new alternative route of synthesis. Structural characterization, bonds, morphology and size were performed by X-ray diffraction (XRD), infrared spectroscopy (IR) and electron microscopy (TEM) and additionally an optical characterization (UV-vis) at room temperature. The XRD study showed that the  $ZnMnO_3$  compound crystallized in a mixed cubic perovskite-wurtzite structure. The IR spectra showed that the compound has energy bands in the  $Mn-O-Mn$  bonds related with octahedral; which is attributed to a vibration characteristic of the perovskite  $ABO_3$  type, addition to find the absorption bands associated with  $Zn-O$  bonds, characteristic of the presence of structural wurtzite hexagonal phase. An estimated size and morphological analysis was carried out by applying the Scherrer's formula and Transmission Electron Microscopy (TEM), revealing non-spherical nanoparticles of 16nm in size. The magnetic measurements  $M(T)$  were performed using zero-field-cooled (ZFC) and field-cooled (FC) protocols revealing a negative Weiss temperature indicating antiferromagnetic behavior with a Néel temperature of 13K. From the optical characterization was possible to get the energy gap at room temperature of  $E_g \cong 2,21eV$ .

**Key words:** Auto-combustion, antiferromagnetic, manganites, nanoparticles, Néel temperature, perovskite, Sol-Gel, Wurtzite.

## INTRODUCTION

Crystallographic phases in  $Zn-Mn-O$  systems have been report generally in two types, hexagonal  $ZnMnO_3$  and tetragonal spinel  $ZnMn_2O_4$  (Saraf et al., 2010).  $ZnMnO_3$  phase is mostly observed in the form of a phase mixture along with  $ZnO$  and  $ZnMn_2O_4$  (Saraf et al., 2010; James et al., 2012). There are few reports of successful synthesis approaches towards  $ZnMnO_3$  (in the mixed phase form) partly because of its instability; relatively

narrower  $Mn$  doping and temperature range for  $ZnMnO_3$  formation (Peiteado et al., 2007; Chamberland et al., 1970). Tetravalent manganese compounds such as  $MnO_2$  and  $AMnO_3$  have been previously reported, while the spinels of  $Mn(IV)$  are rare.  $AMnO_3$  (A=Ca, Ba, Sr, Ni, Co, Zn and Mg) compounds containing  $Mn(IV)$  ions normally crystallize in either the ilmenite (A=Ni, Co, Zn and Mg) or the  $ABO_3$  perovskites structure (A=Ca, Ba and Sr)

\*Corresponding author: E-mail: [enzovha@gmail.com](mailto:enzovha@gmail.com)

Author(s) agree that this article remain permanently open access under the terms of the [Creative Commons Attribution License 4.0 International License](https://creativecommons.org/licenses/by/4.0/)

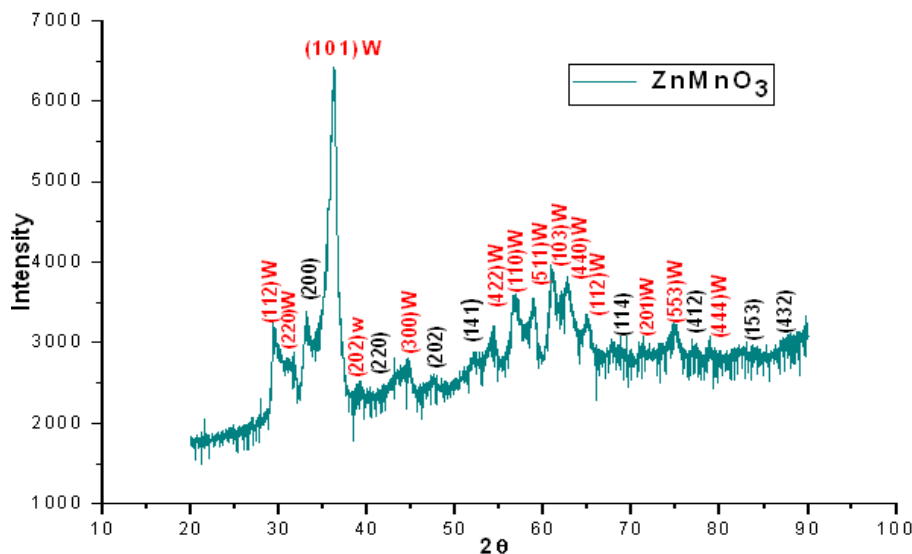


Figure 1. Pattern XRD nanoparticles of  $ZnMnO_3$ .

(Menaka et al., 2011); in which it can have an ideal structure cubic  $P_{m3m}$  space group, orthorhombic  $P_{bnm}$  space group or rhombohedral  $R_{3c}$  space group. The stoichiometry with valence states corresponding to Zinc Manganites  $ZnMnO_3$  is  $A^{+2}B^{+4}O_3^{-2}$ , assigning a cubic unit cell body-centered, bcc, whose center  $Zn^{+2}$  cation is placed;  $Mn^{+4}$  cations occupying the eight vertices of the cell and the anions bcc  $O^{-2}$  occupy the mid-points between the cations  $B$ , in the middle of the edges of the bcc cell (Varshney and Kaurav, 2004; Ghosh et al., 2007).

Here the authors present synthesis, X-Ray diffraction (XRD) and magnetic measurements  $M(T)$  of the  $ZnMnO_3$  nanoparticles system of the mixed cubic structure, perovskite-wurtzite. The results of detailed magnetic  $M(T)$  studies show an antiferromagnetic behavior with  $T_N = 13K$ , behavior reported very recently (Menaka et al., 2011; Jacimovic et al., 2011). Nevertheless, ferrimagnetic behavior has also been reported in  $ZnMnO_3$  nanoparticles with a Néel temperature of 20 K (James et al., 2012); in previous years, Saraf et al. (2010) reported sol-gel synthesis of nanoparticles of cubic  $ZnMnO_3$  with  $D = 30$  nm as size using nitrates method but without reporting any magnetic investigations. The synthesis of a cubic  $ZnMnO_3$  nanoparticles was also reported by Toussaint (1964), but again without magnetic characterization (Toussaint, 1964). Recently, Jacimovic et al. (2011) reported the synthesis of cubic  $ZnMnO_3$  nanoparticles by using nitrates, they observed splitting of the zero-field-cooled (ZFC) and field-cooled (FC) magnetization data at 15 K; however, no additional details of its magnetic behavior were reported. Therefore, further research is recommended to fully understand the nature of magnetism in  $ZnMnO_3$  nanoparticles.

## Synthesis

$ZnMnO_3$  nanoparticles systems were synthesized by the sol-gel auto-combustion method (Seminario, 2012; Munir and Holt, 1987; Chinarro et al., 2005). The precursors used were Manganese (II) Nitrate,  $Mn(NO_3)_2 \cdot 4H_2O$  and Zinc Nitrate,  $Zn(NO_3)_2 \cdot 6H_2O$ ; both were easily dissolved in distilled water and stirred for 5 minutes at room temperature. On the other hand, citric acid  $C_6H_8O_7 - H_2O$  was used as organic fuel (combustion heat of  $C_h = 18.3$  KJ, which is easily dissolved in distilled water, stirred at room temperature for 10 min. All solutions were made separately until get a completely clear solution; then they were mixed and kept under stirring of all precursors already dissolved in a beaker on a hotplate at  $85^\circ C$  for 4 h until the final product has a viscous and yellow appearance. After this, the sol-gel product was deposited in a shuttle glass and the center of a tube furnace preheated to  $500^\circ C$ . The furnace is slightly inclined to produce a slight convection that allows the air circulation at the time at which combustion occurs. A few seconds after introducing the sol-gel in oven, violent flames pointing appearance was observed that the self-combustion process had occurred; this releases large amounts of gases. Just when the material stops emitting gases, about 3 min after entering the material in the oven, the furnace was turned off and allowed to cool to room temperature. It is noted that grayish white foam was obtained. The material it was removed from shuttle glass (when there is combustion the material that is out of the shuttle glass is discarded, only material left inside the shuttle glass after combustion is used) and ground gently on agate stone. Thus  $ZnMnO_3$  nanoparticles were obtained.

## RESULTS AND DISCUSSION

$ZnMnO_3$  nanoparticles were characterized by X-Ray diffraction without further treatment. The diffractogram obtained at room temperature is shown in Figure 1. This was identified as a mixed cubic perovskite-wurtzite structure, where eight perovskite phase peaks are observed; (200), (220), (202), (141), (114), (412) (153)

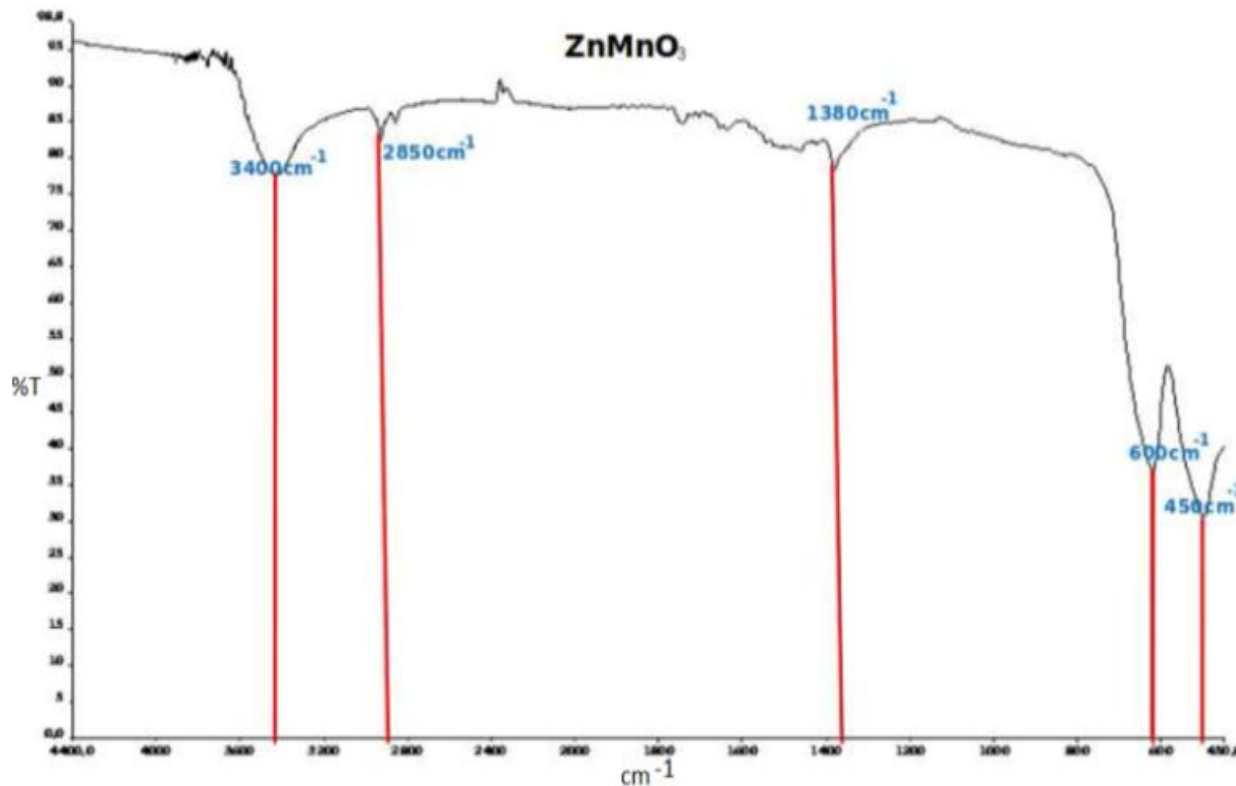


Figure 2. FT-IR spectra for  $ZnMnO_3$ .

and (432) peaks plus fourteen wurtzite phase; (112), (220), (101), (202), (300), (422), (110), (511), (103), (440), (112), (201) (553) and (444). He also proceeded to compare the experimental diffraction pattern with the diffraction pattern of the reference (Saraf et al., 2010) and the JCPDS card #19-1461. Those reports said that the crystal structure of the  $ZnMnO_3$  compound is a cubic structure face centered of  $P_{m\bar{3}m}$  space group with 8.35 Å and 8.34 Å lattice parameters respectively. For the crystallographic study we use NBS-L program to calculate the value of the lattice parameter, the calculated value was  $a = 8.3488$  Å. By using the diffraction pattern, peak (101), was carried out grain size estimation by applying the Scherrer's formula to throw a value of  $D_S = 18$  nm.

Figure 2 shows FT-IR spectra of the  $ZnMnO_3$  nanoparticles. In these spectra there are five absorption bands, three around 450, 600 and 3400  $cm^{-1}$  in which the absorption band at 450  $cm^{-1}$  corresponds to the  $Zn-O$  bonds, characteristic of the presence of hexagonal wurtzite structural phase. The band at 600  $cm^{-1}$  is attributed to the vibration of  $Mn-O-Mn$  bonds perovskite  $ABO_3$  type (Coey et al., 1999; LiK et al., 1997). The absorption band at 3400  $cm^{-1}$  corresponds to  $O-H$  stretching vibrations (water). The water present in the samples can result from those compounds are hygroscopic. Finally, two smaller bands around

2850  $cm^{-1}$  corresponding to bonds  $C-O_2$ , combustion residues and the band at 1380  $cm^{-1}$ , which suggests the presence of  $N-O$  vibrations could be residues of nitrate source (Wang et al., 2005; Giri et al., 2010; Wade, 2005).

Figure 3 shows an image of  $ZnMnO_3$  sample taken with a transmission electron microscope (TEM) with full scale 20 nm. It may be observed that the nanoparticles have an undefined shape (Although micrograph quality could take the necessary information). This is related to the synthesis used, since the self-combustion is not performed in the total thermal equilibrium; the temperature in different parts of the sample to the flame appear at the time of combustion can be quite different, so it may cause a distribution of grain sizes of the obtained material. Attached at the bottom of fig 3 we show the graph of frequency versus particle diameter obtained from  $ZnMnO_3$  micrograph, of which was fitted with a Gaussian bell-type displays. This allowed us to estimate an average particle size of  $D_{TEM} = 16$  nm. This value is consistent with Scherrer's formula value for the size distribution the diameter of about 120 identifiable particles it was measured in the  $ZnMnO_3$  micrograph to make a statistical data. The particle sizes were taken by hand using a scale ruler who brings the IMAQ-Vision Builder program that comes with its own micrographs. As the particle shape is not spherical, several measurements of particle diameters (between 4 and 5 values) were

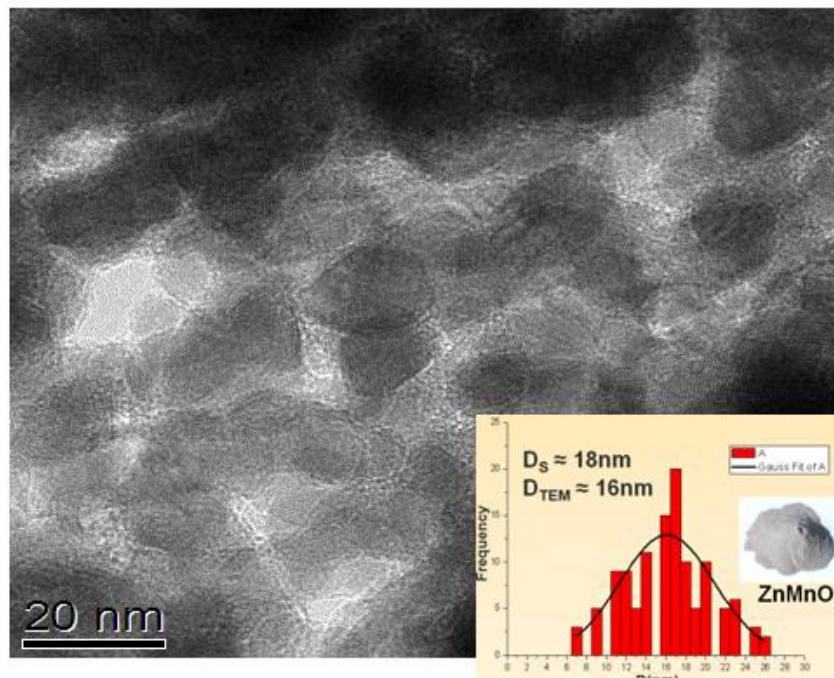


Figure 3. TEM micrographs of  $ZnMnO_3$  and size distribution.

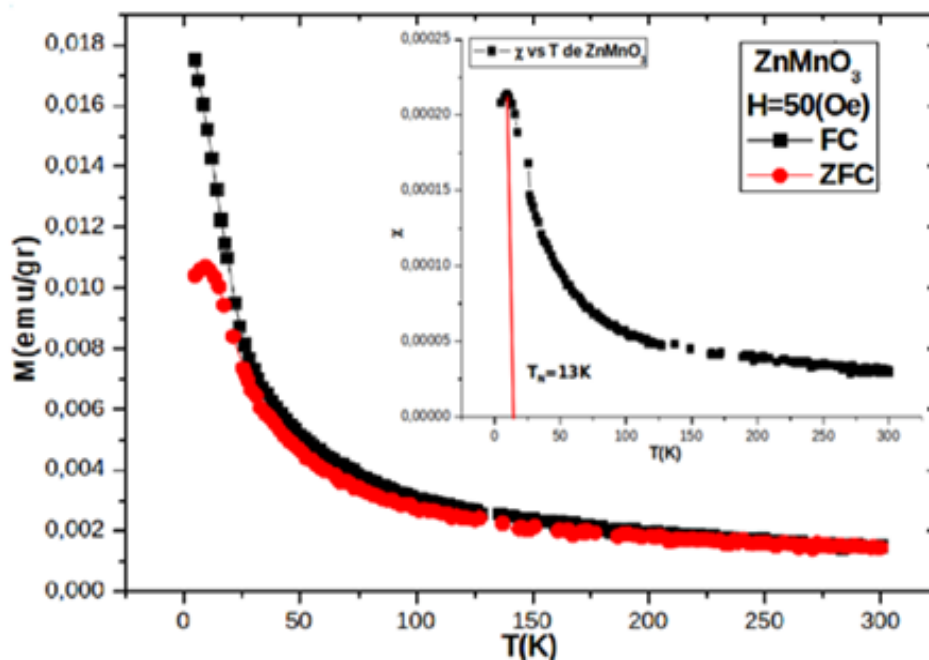


Figure 4. Temperature dependence of the magnetizations for  $ZnMnO_3$  nanoparticles.

made to have a simple average for each particle diameter.

Figure 4 shows the  $M$  vs  $T$  graph of  $ZnMnO_3$  nanoparticles; measured with ZFC and FC protocols in

the temperature range of 5 K to 300 K. It can also be observe an irreversibility temperature,  $T_{irr}$ , at 160 K. In the ZFC curve a transition zone is observed at low temperatures suggesting that we could be approaching to



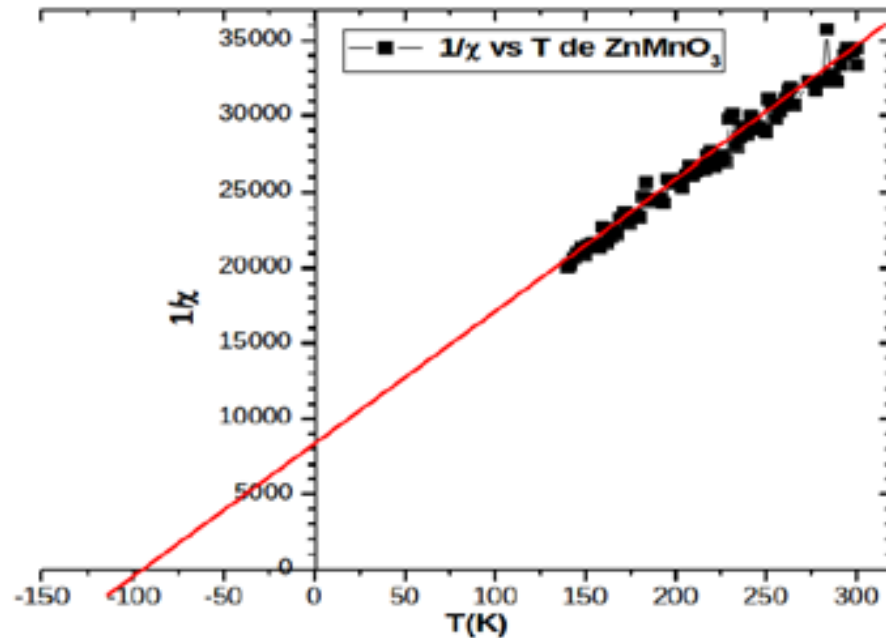


Figure 5.  $1/\chi$  vs  $T$  for nanoparticles of  $ZnMnO_3$ .

some magnetic ordering. The ZFC-FC magnetization curves, presented in fig 4, taken at low temperature, show that there are an AFM transition at 13 K, taken as Neel temperature  $T_N$ , see inset of Figure 4, in agreement with previous determination. Notice that for  $T \leq T_N$  the curves ZFC and FC are widely separated. In the paramagnetic region,  $T \geq T_N$  shown in inset of Figure 4, the magnetic susceptibility;  $M/H = \chi$  versus temperature follow the Curie-Weiss law:  $\chi = C/(T - \theta)$  where the constant  $C$  and the paramagnetic Curie temperature  $\theta$  may be obtained by using the linear behavior presented in fig 5. From the fit of  $1/\chi$  vs  $T$  in the range of 130 to 300 K temperature,  $\theta = -98$  K was obtained.

Figure 5 shows the  $1/\chi$  vs  $T$  taken from FC data. The negative value of  $\theta$  is in agreement with the antiferromagnetic magnetic interaction which is expected in these type of materials  $Zn^{+2}Mn^{+4}O_3^{-2}$  (Menaka et al., 2011; Jacimovic et al., 2011); in which  $Mn$  has a valence state causing only bonds  $Mn^{+4} - O^{-2} - Mn^{+4}$  which show a magnetic super-exchange interaction. The experimental value of the effective magnetic moment obtain from the fit of the constant  $C$  was  $\mu_{eff-ex} = 3.72 \mu_B$  which is close to the theoretical value of the effective magnetic momentum  $\mu_{eff-teo} = 3.81 \mu_B$  (Coey et al., 1999; Arbuza et al., 2008). The small discrepancy between the theoretical value and the experimental effective magnetic moment may be due to the fact that this sample has a mixed perovskite-wurtzite structure; mainly because the presence of wurtzite crystalline phases of  $ZnO$ .

Figure 6 shows the UV-vis optical absorption graph of

$ZnMnO_3$  nanoparticles. For the optical measurements, a pellet of mass 1.5 g with composition of 90% of  $ZnMnO_3$  and 10%  $KBr$  make, the pellet is homogeneous in consistency. This mixture was brought into a press with a circular mold where it was subjected to a pressure of  $10 T/cm^2$ , obtaining a thickness 0.65 mm pad. The optical absorption spectrum was taken at room temperature. The energy gap value was estimated using the relationship:  $\alpha h\nu = A(h\nu - E_g)^{1/2}$ . Where  $h\nu$  is the photon energy,  $\alpha$  is the absorption coefficient, ( $\alpha = A_\lambda/d$ ), where  $A_\lambda$  is the absorbance and  $d$  is the thickness of sample pellet,  $E_g$  is the energy gap and  $A$  a constant. The direct energy gap can be obtained from the extrapolation of straight line to  $(\alpha h\nu) = 0$  as is shown in fig 6. For the UV-vis optical absorption graph analysis measure, the absorption coefficient  $\alpha$ , for different nominal values of  $x$  was calculated and plotted as a function of incident photon energy (Jacimovic et al., 2011) at room temperature. This shows that there is a region close to a linear behavior in the region between 2.5 eV and 3.5 eV. The main edge is constituted by a  $E_g \cong 2.21 eV$  direct transition value. Then, the quadratic dependence of the product of the absorption coefficient with the energy of the incident photon is obtained. Before starting with the analysis of the result, we mention that the results obtained for the  $ZnMnO_3$  sample is the direct transition analogous to the  $ZnO$ ; because it has been taken as a reference to  $ZnO$ ,  $Zn_{(1-x)}Mn_{(x)}O$  and  $ZnMn_2O_4$  (Pan et al., 2011; Rivas, 2012) in the analysis of optical absorption for zinc manganite  $LaMnO_3$ , because there are few reports

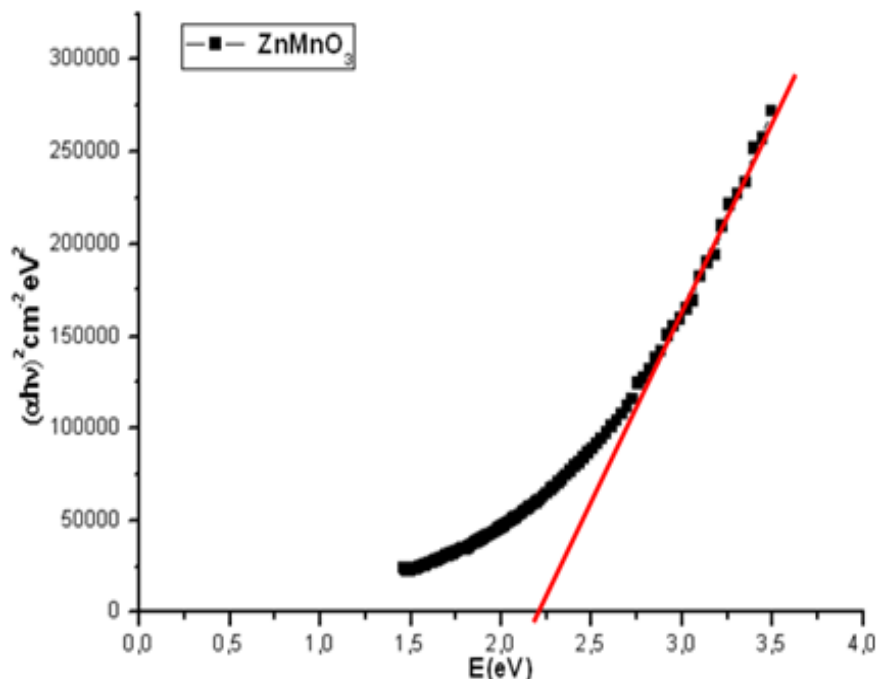


Figure 6. Room temperature at  $(\alpha hv)^2 vs E(hv)$ .

on the optical absorption of this type of nanoparticles about it. It is assumed that this work is one of the pioneers in the study of the optical absorption of zinc manganite nanoparticles. Considering the reflectivity of the material, with a low absorption of the curve is set to zero, which is a translational axis; furthermore, a high absorption was observed possibly residual defects in the structure of the material, and/or the existence of other phases, etc. Under the experimental conditions which measurements were made, the value of direct energy gap from the reported values regarding Zinc Oxide  $E_g \cong 3.40 eV$  that speak of a decline in the value of the energy gap when the Zinc Oxide is Manganese doped,  $Zn_{0.97}Mn_{0.03}O$  in thin films; and in Zinc and Manganese Ferrites,  $Mn_{(x)}Zn_{(1-x)}Fe_2O_4$ , with a energy gap value about  $E_g \cong 2.28 eV$ ; whose values, especially the latter is the closest to those reported in this work (Pan et al., 2011; Rivas, 2012).

## CONCLUSIONS AND RECOMMENDATIONS

For the  $ZnMnO_3$  as grown nanoparticles we found a mixed cubic perovskite-wurtzite structure *fcc* with lattice parameters  $a = 8.3488 \text{ \AA}$ . FT-IR show the absorptions band at  $650 \text{ cm}^{-1}$  associated with the perovskites and the absorption band at  $450 \text{ cm}^{-1}$  corresponding to the  $ZnO$  bounds characteristic for the presence of structural wurtzite hexagonal phase; this is consistent with the

information obtained from X-ray diffraction. In the  $ZnMnO_3$   $M vs T$  magnetic measurement was found indicating  $\theta_w = -98 K$  antiferromagnetic behavior associated with super exchange interaction, consistent with the majority of reports of such materials; in which  $Mn$  has only one valence state. The optical measurements yielded a  $E_g \cong 2.21 eV$  direct energy value of energy gap. It is recommended to continue the study of the magnetic properties with  $M vs H$  measurements at different temperatures to examine whether there maybe super paramagnetism and  $M vs T$  measurements on alternate fields at different frequencies in a temperature range around the  $T = 13 K$  to examine whether some behavior of spin glass is presented and synthesize the  $ZnMnO_3$  nanoparticles system following other synthesis methods.

## Conflict of Interest

The authors have not declared any conflict of interest.

## ACKNOWLEDGEMENTS

The authors are grateful to CDCHTA –ULA for funding the project C-1658-09-05-A. Also grateful to C. Pernechele and F. Rossi, Dipartamenti di Fisica, CNISM, Universita di Parma, A-1-43100, Italia, and IMEM-CNR Institute, 43019, Parma Italia respectively for experimental collaboration towards the study.

## REFERENCES

- Arbuzova TI, Gizhevskii BA, Zakharov RG, Petrova SA, Chebotaev NM (2008). Magnetic susceptibility of Nanostructural Manganite  $LaMnO_{2+z}$  Produced by Mechanochemistry Method. *Phys. Solid State* 50(8):1487-1494.
- Chamberland BL, Sleight AW, Weiher JF (1970). Preparation and Characterization of  $MgMnO_3$  and  $ZnMnO_3$ . *J. Solid State Chem.* 1:512.
- Chinarro E, Chinarro E, Moreno B, Martin D, González L, Villanueva E, Guinea D, Jurado JR (2005). Posibilidades del Análisis de Imagen para el Estudio de la Síntesis de Materiales por Combustión. *Bol. Soc. Esp. Ceram.* 44(2):105-112.
- Coey JMD, Viret M, Von Molnar S (1999). Mixed-Valence Manganites. *Adv. Phys.* 48:167.
- Ghosh S, Sharma AD, Basu RN, Maiti HS (2007). Influence of B Site Substituents on Lanthanum Calcium Chomite Nanocrystalline Materials for a Solid-Oxide Fuel Cell. *J. Am. Ceram. Soc.* pp. 3741-3747.
- Giri A, Makhil A, Ghosh B, Raychaudhuri AK, Kumar S (2010). Functionalization of manganite nanoparticles and their interaction with biologically relevant small ligands: Picosecond time-resolved FRET studies. *Pal. Nanoscale* 2:2704-2709.
- Jacimovic J, Mickovic Z, Gaal R, Smajda R, Vajie C, Sienkiewicz A, Ferro L, Magrez A (2011). Synthesis, Electrical resistivity, Thermo-Electric Power and Magnetization of Cubic  $ZnMnO_3$ . *Solid State Commun.* 151:487.
- James DR, Thota S, Kumar J, Seehra MS (2012). Synthesis, Structure and Magnetic Behavior of nanoparticles of Cubic  $ZnMnO_3$ . *Appl. Phys. Lett.* 100:252407.
- LiK KB, Li XJ, Zhu KG (1997). Infrared Absorption spectra of Manganese Oxides  $La_{1-x-y}R_yCa_xMnO_3$ . *J. Appl. Phys.* 10:6943.
- Menaka SL, Samal KV, Ramanujachary SE, Lofland G, Ganguli AK (2011). Stabilization of Mn(IV) in Nanostructured Zinc Manganese Oxide and Their Facile Transformation from Nanospheres to Nanorods. *J. Mater. Chem.* 21:8566.
- Munir ZA, Holt JB (1987). The combustion synthesis of refractory nitrides. *Theoretical-Analysis. J. Mater. Sci.* 22(2):710-714.
- Pan Z, Xinyong L, Qidong Z, Shaomin L (2011). Synthesis and optical property of one-dimensional spinel  $ZnMn_2O_4$  nanorods. *Nanoscale Res. Lett.* 6:323.
- Pankove J (1971). *Optical Processes in Semiconductor*. Dover Publications. New York. First Edition.
- Peiteado M, Caballero AC, Makovec D (2007). Phase Evolution of  $Zn_{1-x}Mn_xO$  system synthesized via oxalate precursors. *J. Eur. Ceramic Soc.* 27:3915.
- Rivas P (2012). Tesis de Lic. En Física. Universidad de los Andes, Venezuela.
- Saraf LV, Nachimuthu P, Engelhard M H, Baer DR (2010). Stabilization of  $ZnMnO_3$  phase from sol-gel synthesized nitrate precursors. *J. Sol-Gel. Sci. Technol.* 53:141-147.
- Seminario (2012). *Métodos de Preparación de nanopartículas*. Edgar Pérez, Universidad de los Andes, Mérida Venezuela, 2012.
- Toussaint H (1964). *Revue de chimie minérale. Revue für anorganische Chemie. Inorganic chemistry review.* 1:141.
- Varshney D, Kaurav N (2004). Analysis of low temperature specific heat in the ferromagnetic state of the Ca-doped manganites. *Eur. Phys. J. B.* 37:301-309.
- Wade LG (2005). *Química Orgánica. 5 edición.* <http://www.slideshare.net/alis590/quimica-organica-wade-5ta-edicion>.
- Wang H, Zhao Z, Xu C-M, Liu J (2005). Nanometric  $La_{1-x}K_xMnO_3$  Perovskite-type oxides-highly active catalysts for the combustion of diesel soot particle under loose contact conditions. *Catal. Lett.* 102:5864.